CHARACTERISTICS OF SOFT SOLAR X-RAY BURSTS

JERRY F. DRAKE*

Dept. of Physics and Astronomy, The University of Iowa, Iowa City, U.S.A.

(Received in final form 14 August, 1970)

Abstract. The burst component of the solar X-ray flux in the soft wavelength range $2 < \lambda < 12$ Å observed from Explorer 33 and Explorer 35 from July 1966 to September 1968 was analyzed. In this period 4028 burst peaks were identified.

The differential distributions of the temporal and intensity parameters of the bursts revealed no separation into more than one class of bursts. The most frequently observed value for rise time was 4 min and for decay time was 12 min. The distribution of the ratio of rise to decay time can be represented by an exponential with exponent -2.31 from a ratio of 0.3 to 2.7; the maximum in this distribution occurred at a ratio of 0.3. The values of the total observed flux, divided by the background flux at burst maximum, can be represented by a power law with exponent -2.62 for ratios between 1.5 and 32. The distribution of peak burst fluxes can be represented by a power law with exponent -1.75 over the range 1–100 milli-erg $(\text{cm}^2\ \text{sec})^{-1}$. The flux time integral values are given by a power law with exponent -1.44 over the range 1–50 erg cm^{-2}.

The distribution of peak burst flux as a function of Hα importance revealed a general tendency for larger peak X-ray fluxes to occur with both larger Hα flare areas and with brighter Hα flares. There is no significant dependence of X-ray burst occurrence on heliographic longitude; the emission thus lacks directivity.

The theory of free-free emission by a thermal electron distribution was applied to a composite quantitative discussion of hard X-ray fluxes (data from Arnoldy *et al.*, 1968; Kane and Winckler, 1969; and Hudson *et al.*, 1969) and soft X-ray fluxes during solar X-ray bursts. Using bursts yielding measured X-ray intensities in three different energy intervals, covering a total range of 1–50 keV, temperatures and emission measures were derived. The emission measure was found to vary from event to event. The peak time of hard X-ray events was found to occur an average of 3 min before the peak time of the corresponding soft X-ray bursts. Thus a changing emission measure during the event is also required. A free-free emission process with temperatures of $12\text{–}39 \times 10^6$ K and with an emission measure in the range 3.6×10^{47} to 2.1×10^{50} cm^{-3} which varies both from event to event and within an individual event is required by the data examined.

1. Introduction

Solar X-rays in the range 2–12 Å (1–6 keV) have been monitored by University of Iowa detectors on the earth orbiting satellite Explorer 33 (since July 1966) and on the lunar orbiting satellite Explorer 35 (since July 1967). The detector complements consisted of three Geiger-Mueller tubes on Explorer 33 and one Geiger-Mueller tube on Explorer 35. An in-flight calibration technique was used to normalize all fluxes to a common standard. It was additionally possible to obtain the *absolute* value of the flux, essentially independent of assumed temperature (Van Allen, 1967a). The instrumentation and data reduction are described in detail elsewhere (Drake *et al.*, 1969).

A procedure was developed to identify and parameterize the burst component of the flux by computer. Burst parameter distributions were formed and, in most cases, fit with empirical relations. The Hα flare and X-ray burst occurrence statistics were

* Now at Department of Astrophysical Sciences, Princeton University, Princeton, New Jersey.

Solar Physics **16** (1971) 152–185.

obtained. The X-ray burst heliographic longitude distribution was determined to test the possibility of directional emission. A quantitative intercomparison was made with harder X-ray burst data and with the assumption of free-free emission to determine the behavior and values of both temperature and emission measure as evidenced by the 1–6 keV flux.

2. Theory

The flux in the range 2–12 Å received at the earth's orbit due to free-free emission from the surface of the sun is (Drake, 1970; Gibson, 1969)

$$F(2\text{–}12\ \text{Å}) = 8.58 \times 10^{-49}\, S\, T^{-1/2} \exp(-12/T), \tag{1}$$

where F is in units of milli-erg $(\text{cm}^2\ \text{sec})^{-1}$, T is in units of 10^6 K, and S, the emission measure, is in units of cm^{-3}.

The flux is a function of two parameters, S and T. If it is assumed that both the temperature and emission measure are the same for differing, but adjacent, photon energy intervals, then two simultaneous measurements quantitatively establish the temperature and emission measure.

Three flare models are pertinent to this study. De Jager and Kundu (1963) proposed a model whose pertinence is that accelerated electrons move radially in the solar atmosphere whereas in the model of Takakura and Kai (1966) energetic electrons move approximately parallel to the solar surface. The third flare model (Carlquist, 1968) is concerned primarily with the production of the energetic particles needed in the previous models.

Energetic electrons in the first two models have preferred directions of motion. Elwert (1968) pointed out that if this were true and non-thermal bremsstrahlung produced the rise and maximum of the X-ray burst, then the heliographic longitude distribution of X-ray bursts might distinguish between the two flare models.

3. Burst Identification Procedure

A program was developed to both identify the occurrence of an X-ray burst and determine several of the burst parameters. The adopted program compares, at each data point, the flux value to a background flux value which has been determined manually. When the ratio of the observed flux to the background flux exceeds an assigned value, a burst is recorded and its parameters are determined. The arbitrary value for the ratio was adopted as 1.5 after trying several values from 1.25 to 4.0.

The burst parameters obtained and their method of determination can best be discussed by examining a sample page of the burst output listing, as shown in Figure 1. The beginning time of the burst is the interpolated time when the rising flux curve equals the local background flux plus 20% of the peak flux increase above background. The year, month, and day of month of the beginning time are recorded in the first three colums. The next three columns are the beginning time in hours, minutes, and seconds.

BEGIN			PEAK	END	PEAK		TIME			SUMF	R/D	R/T	D/T	TLOS
YY MON DD	HH MM SS	HH MM SS	HH MM SS	VALUE	RATIO	GAPS	RISE	DECAY	TOTAL					
67 MAY 25	17 2 53#	17 8 21	17 29 28	2.05	1.589	0	0 5 27	0 21 7	0 26 35	1.782	0.26	0.21	0.79	0.000
67 MAY 25	19 28 34	19 46 31	20 4 42	5.30	2.511	0	0 17 57	0 18 11	0 36 9	6.311	0.99	0.50	0.50	0.000
67 MAY 25	20 47 11	20 54 41	21 20 52	3.67	2.040	0	0 7 30	0 26 11	0 33 41	4.768	0.29	0.22	0.78	0.000
67 MAY 25	22 22 7U	0 8 19U 0 43 46	2 14 24U	4.78 3.65	2.339 2.019	6D	1 46 12	1 30 38	3 52 17	11.418	1.17	0.46	0.39	0.904
67 MAY 26	12 35 51	12 40 58	12 52 29	8.94	3.401	0	0 5 7	0 11 31	0 16 38	5.937	0.44	0.31	0.69	0.000
67 MAY 26	13 37 15	14 30 3U 16 16 24	21 51 2U	6.55 12.53	2.783 4.453	14B	0 52 48	5 34 38	8 13 47	187.896	0.16	0.11	0.68	0.346
67 MAY 27	0 40 18U	1 57 15U	4 32 49U	8.85	3.723	4R	1 16 57	2 35 34	3 52 31	11.700	0.49	0.33	0.67	0.800
67 MAY 27	5 14 0U	5 43 35U	6 23 12	10.50	4.199	5D	0 29 35	0 39 37	1 9 13	10.387	0.75	0.43	0.57	0.621
67 MAY 27	11 53 48U	12 35 22 13 38 6 15 24 26	15 50 6	2.25 2.40 1.93	1.722 1.775 1.622	10B	0 41 34	0 25 40	3 56 18	13.986	1.62	0.18	0.11	0.273
67 MAY 27	23 3 49	23 16 13	23 30 54U	4.31	2.407	2D	0 12 25	0 14 40	0 27 5	3.617	0.85	0.46	0.54	0.334
67 MAY 28	0 27 51	0 38 2U	0 50 2	24.78	9.108	2D	0 10 11	0 12 0	0 22 11	17.606	0.85	0.46	0.54	0.445
67 MAY 28	5 40 5U	5 51 38	6 20 43U	333.70	110.632	3R	0 11 33	0 29 5	0 40 37	478.266	0.40	0.28	0.72	0.333
67 MAY 28	7 21 37#	7 57 4	9 44 58	11.57	4.697	6B	0 35 27	1 47 53	2 23 20	50.090	0.33	0.25	0.75	0.359
67 MAY 28	21 31 3	22 7 54 0 18 48	3 26 12	2.67 2.54	1.746 1.849	13B	0 36 51	3 7 24	5 55 9	21.333	0.20	0.10	0.53	0.282
67 MAY 29	4 16 58U	5 2 25U	5 31 27U	2.21	1.762	4	0 45 27	0 29 2	1 14 29	0.877	1.57	0.61	0.39	1.000
67 MAY 29	9 36 32	9 40 34U	9 53 6	1.62	1.576	1	0 4 2	0 12 33	0 16 35	0.480	0.32	0.24	0.76	0.571
67 MAY 29	14 19 36	14 29 38	14 49 29	1.38	1.549	0	0 10 2	0 19 51	0 29 54	1.480	0.51	0.34	0.66	0.000
67 MAY 29	14 59 54	15 2 21	15 9 50	1.73	1.688	0	0 2 27	0 7 29	0 9 56	0.643	0.33	0.25	0.75	0.000
67 MAY 29	18 51 53	19 7 47	19 45 19	3.50	2.389	1D	0 15 54	0 37 33	0 53 26	6.779	0.42	0.30	0.70	0.100
67 MAY 29	21 11 51	22 18 40	22 38 28	3.11	2.236	1R	1 6 49	0 19 48	1 26 37	5.981	3.37	0.77	0.23	0.152
67 MAY 29	22 45 43#	23 18 40	0 11 2	3.19	2.266	2B	0 32 56	0 52 22	1 25 18	6.626	0.63	0.39	0.61	0.152
67 MAY 30	2 24 35	2 29 34	2 38 57U	1.33	1.529	1	0 4 58	0 9 23	0 14 21	0.967	0.53	0.35	0.65	0.286
67 MAY 30	4 8 6	4 21 22 8 45 53	10 23 50	2.45 4.15	1.971 2.647	11D	0 13 16	1 37 57	6 15 44	22.804	0.14	0.04	0.26	0.275
67 MAY 30	17 27 56	17 34 55	17 53 53	6.14	3.313	0	0 6 59	0 18 58	0 25 57	5.892	0.37	0.27	0.73	0.000

Fig. 1. Sample page from the 2–12 Å X-ray burst listing. The description by columns is given in the text (Section 3).

The time, in hours, minutes, and seconds, under 'Peak' corresponds to the time of the maximum flux of the burst. The ending time is the interpolated time when the falling flux curve equals the local background flux plus 20% of the peak flux increase above background and appears under 'End' in units of hours, minutes, and seconds. All times used have been corrected to correspond to the central time of the flux sampling period. A 'U' on a beginning, peak, or ending time indicates that the time is uncertain because the corresponding data point was in or on the edge of a data gap. A record mark on a beginning (ending) time indicates that the time value was not determined by the previously discussed interpolation scheme because another burst occurred before (after) the flagged time so that the flux was never small enough to meet the interpolation requirement. In this case the flagged time corresponds to the time of the minimum flux attained.

A burst is listed as one burst with two peaks if after the first peak the flux decreased to a value less than 80% of the total flux value at the time of the first peak and then increased again to a value equal to, or exceeding, the total flux at the time of the first peak. This procedure can be repeated to produce multiply peaked bursts. In cases of

multiply peaked bursts, the beginning time is determined from the first peak and the ending time from the last peak in the interpolation previously described.

Examples illustrating the determination of start, peak, and end times under a variety of complicating conditions are shown in Figure 2. In the 23 May events the first burst does not reach an end time by the usual interpolation method; the start time of the third event is also not determined by interpolation. Again in the 28 May events the start time of the second burst is not determined by interpolation and is accordingly marked with a record mark in the listing shown in Figure 1.

The column in Figure 1 under 'Peak Value' lists, in units of milli-erg $(cm^2\ sec)^{-1}$, the flux increase above the background level for the maximum flux in the burst. The

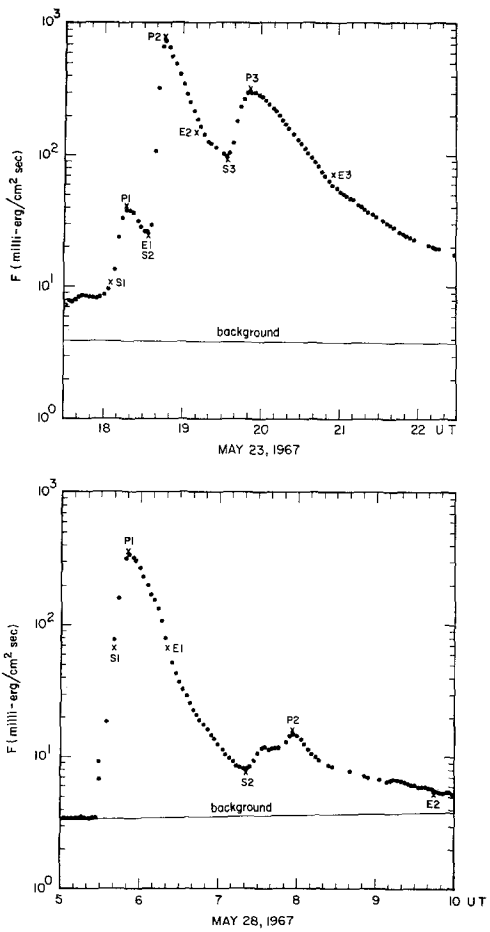

Fig. 2. Sample X-ray bursts with computer determined start (S), peak (P), and end (E) times for several cases which include complications in these determinations. The events in each of the two illustrations are labeled consecutively after the designation of start, peak, or end time; for example, P2 is the peak time of the second burst. The 28 May events correspond to the tabular data given in Figure 1.

ratio of the maximum flux to the background flux appears in the column 'Ratio'. The number of data losses of five consecutive minutes or more which occurred during the burst are recorded under the heading 'Gaps'.

The rise time, decay time, and total duration of the burst appear under the broad heading of 'Time' under the appropriate subheadings. These values are determined directly from the beginning, peak, and ending times.

The time integral of the flux increase above the background level for the burst is listed in the column 'Sumf' in units of erg cm^{-2}. The flux is summed from the beginning time to the ending time of the burst. The contributions to the integral occurring before the beginning time and after the ending time were obtained, to a first approximation, by a triangular extrapolation formula based on the two data points nearest to each end. The tabulated value appearing is thus once corrected.

The columns headed by 'R/D', 'R/T', and 'D/T' list the ratios of rise time to decay time, rise time to total burst duration, and decay time to total burst duration, respectively.

The final column, 'Tlos', contains the ratio of the time lost in gaps to the total time of the burst. This value can range from 0.000 for complete coverage to 1.000 if each point in the burst is on the edge of a gap. The non-zero values given in this column can provide an approximate correction to the flux time integral values to partially compensate for the contribution to the integral lost during a gap.

The results of the computer analysis were examined together with the graphical form of the data for each listed burst to eliminate, or identify, listings which desagree significantly for a subjective, visual impression of the plotted data for the event. Less than 10% of the bursts were in disagreement by this test. Bursts in question were analyzed by hand and the resulting parameters substituted for the erroneous ones.

A total of 3515 bursts and 513 secondary burst peaks were listed in this manner for the time interval 2 July 1966 to 18 September 1968 for a total of 4028 burst peaks. Based on the data from August 1967 through August 1968 there was an average of 8 bursts per day.

4. Burst Parameter Distributions

As a listing on magnetic tape had been produced containing both the parameters for each burst and information detailing the quality of the burst (if and where in the burst a data gap had occurred), the distribution of parameters was also obtained by computer. Only events of best quality in each parameter were used; the exclusion of events in each category will be discussed with each parameter distribution.

A. RISE TIME

No rise times were included which were based on a flagged beginning or peak time or for which there was a data gap between the beginning and peak times. The number of events passing these criteria was 2206. Figure 3 shows the distribution of 94% of the events with good quality rise times. The number of events in each class, the number of those events shown on the corresponding plot, and the percentage of the total number

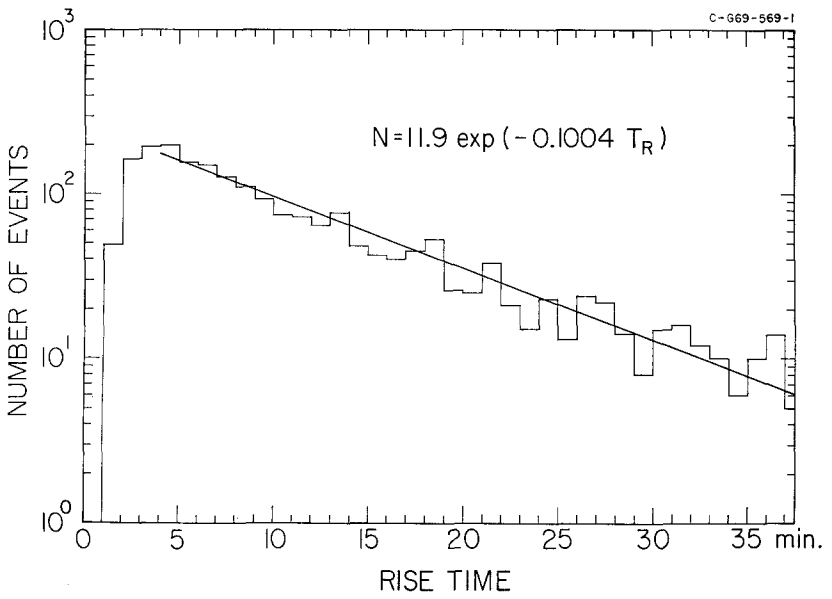

Fig. 3. Differential distribution of 2–12 Å X-ray bursts with respect to rise time. The straight line is a least-squares fit over the region indicated.

of events in each class appearing on the plots is given in Table I and will not be specifically stated in the text for the remaining distributions.

The most common rise time was 4 min. A linear least-squares fitting program with weighting equal to the square root of the number of events in each interval was used to fit the data. The data from 4 min to 38 min, comprising 75% of the events in this distribution, are represented by the equation

$$N = 11.9 \exp[(-0.1004 \pm 0.0009)\, T_R]$$
$$T_R \geqslant 4 \text{ min}. \tag{2}$$

TABLE I

Parameter distribution statistics

Parameter	Total number of events in distribution	Number of events in plot	Percentage of events in plot
Rise time	2206	2070	94
Decay time	2227	2059	93
Total time	1586	1426	90
Rise time/total time	1586	1586	100
Decay time/total time	1586	1586	100
Rise time/total time	1626	1598	98
Peak flux/background	3154	3139	99
Peak flux	3154	3140	99
Flux time integral	1586	1185	75

In Equation (2) N is the percentage probability for the occurrence of a burst in the differential interval $T_R \pm 0.5$ min.

The uncertainty expressed in the exponent is the standard deviation of the exponent as determined in the fitting program. The uncertainties expressed for all following exponents determined for parameter distributions were determined in this same manner unless specifically stated otherwise.

B. DECAY TIME

No decay times were included which were determined from flagged peak or ending times, or for which there was a data gap between the peak and ending times. The distribution of decay times obtained is shown in Figure 4. The most common decay

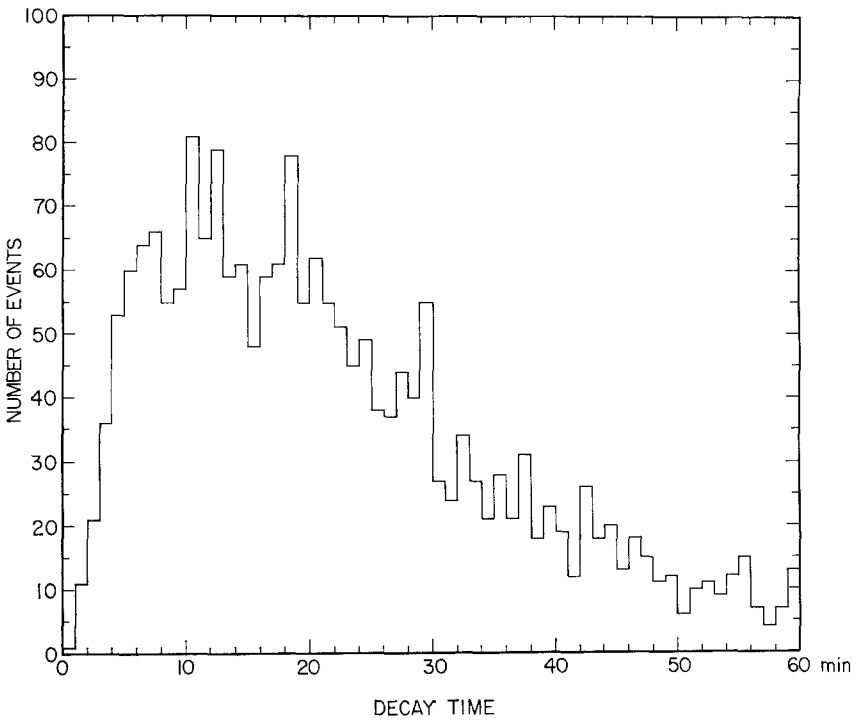

Fig. 4. Differential distribution of 2–12 Å X-ray bursts with respect to decay time.

time is 10–13 min; a nominal value of 12 min will be used henceforth. There is only one significant peak in this distribution at the nominal value of 12 min.

C. TOTAL DURATION

Only bursts continuous at the 5-min interval level and without flagged beginning or ending times were included in this distribution. The total burst duration distribution is shown in Figure 5. A nominal value for the most common burst duration is 16 min

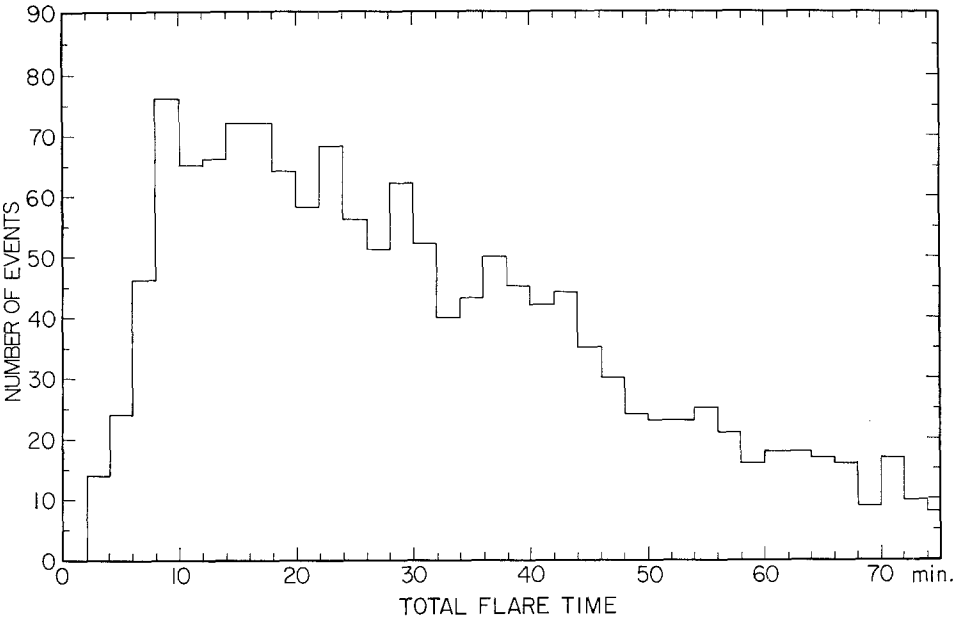

Fig. 5. Differential distribution of 2–12 Å X-ray bursts with respect to the total burst duration; the number of events per 2-min interval is shown.

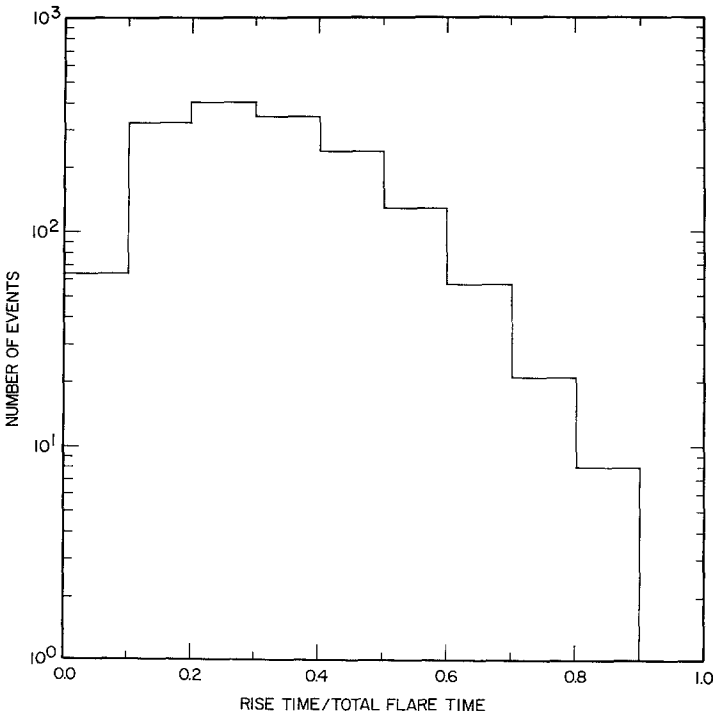

Fig. 6. Differential distribution of 2–12 Å X-ray bursts with respect to the ratio of the rise time to the total burst duration.

although the peak is rather broad (8–24 min). There is no evidence of more than one peak in the total burst duration distribution.

D. RATIO OF RISE TIME TO TOTAL DURATION

Using the same criteria as used before in the rise time, the distribution of bursts with respect to the ratio of the rise time to total duration was determined. The distribution obtained is shown in Figure 6. The solitary peak in this distribution is at 0.25.

E. RATIO OF RISE TO DECAY TIME

The same criteria were again used to define good quality rise and decay times. The distribution of events with respect to the ratio of rise to decay time is shown in Figure

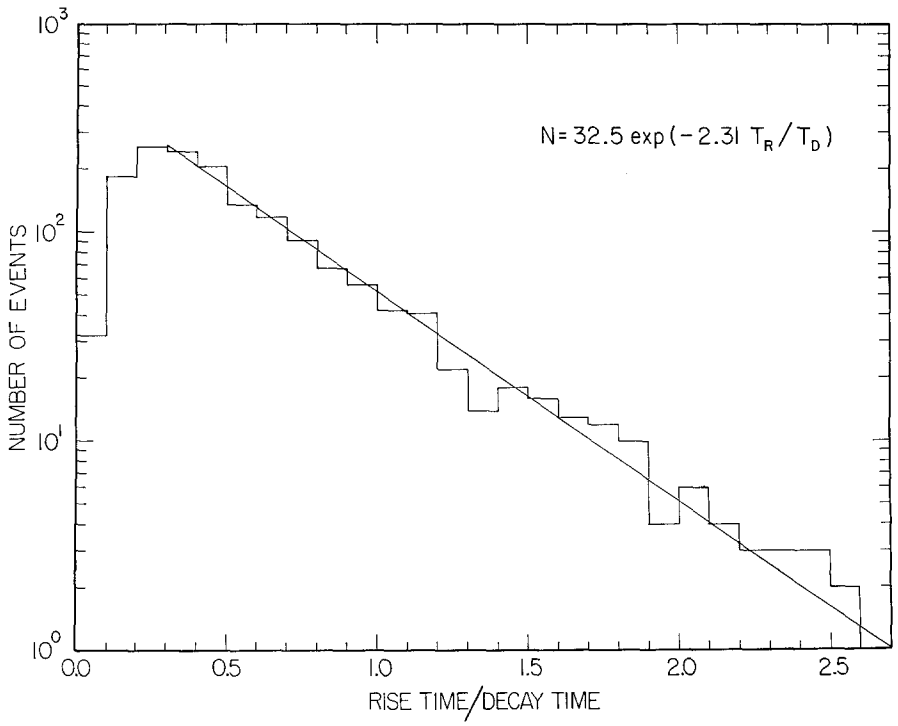

Fig. 7. Differential distribution of 2–12 Å X-ray bursts with respect to the ratio of the rise time to the decay time. The straight line is the least-squares fit over the region indicated.

7. From a ratio of 0.3 to a ratio of 2.7, comprising 69% of the events in this category, the distribution can be represented by

$$N = 32.5 \exp[(-2.309 \pm 0.018)\, T_R/T_D], \tag{3}$$

where N is the percentage of the total number of events in the distribution, per 0.1 interval centered on the ratio of rise to decay time, T_R/T_D. The significant peak in this distribution occurs at a ratio of rise to decay time of 0.3.

F. DISCUSSION OF TEMPORAL PARAMETERS

There is no evidence in the temporal parameters distributions for the existence of more than one class of X-ray burst in the 2–12 Å (1–6 keV) range. More classes may exist but cannot occur for a substantial number of bursts. It appears adequate to consider bursts as being of one standard form with substantial and continuous variability in all parameters. The temporal description of this standard (most common) 2–12 Å burst is a rise time of 4 min, ratio of rise time to total time of 0.25, and ratio of rise time to decay time of 0.3.

These typical values for 1–6 keV bursts may be compared with the values reported for 3.0–4.5 keV bursts and 7.7–12.5 keV bursts. A 10% to 90% rise time and 90% to 10% fall time were given for the typical 3.0–4.5 keV burst by Culhane and Phillips (1969). An e-folding rise and fall time for a typical 7.7–12.5 keV burst was given by Hudson *et al.* (1969). The given rise and decay times were used to compute temporal parameters comparable to those obtained in this study. The comparison of these parameters is presented in Table II. The change in the parameters with increasing

TABLE II

Comparison of derived burst temporal parameters with previously reported values

	Rise time (min)	Decay time (min)	Total duration (min)	Rise time / Decay time	Rise time / Total time	Decay time / Total time
This study (1–6 keV)	4.0	12.0	16.0	0.30	0.25	0.75
Culhane and Phillips (1969) (3.0–4.5 keV)	2.8	6.3	9.1	0.44	0.31	0.69
Hudson *et al.* (1969) (7.7–12.5 keV)	1.4	7.6	9.1	0.19	0.16	0.84

X-ray hardness is immediately evident in the rise time comparison. A decreasing rise time with increasing burst hardness is clearly seen. The trend of the decay time to decrease is clearly seen from the 1–6 keV bursts to harder bursts. The greater total duration of the softer bursts is also clearly seen. For the remaining ratio parameters, the 1–6 keV values in all three cases lie nearly midway between the other two values. As the ratio values are strongly affected by any uncertainty in the rise or decay times, less agreement would be expected among them.

G. FLUX-TO-BACKGROUND RATIO AT BURST PEAK

The distribution for the ratio of total flux to background flux evaluated at burst maximum utilized no events for which the peak intensity occurred on the edge of a data gap, i.e., the maximum intensity was not definitely observed. Since the burst identification criterion was set for a ratio of at least 1.5, the observed number of events in the interval 1.5 to 2.0 was doubled to yield the number for the interval 1.0 to 2.0. The

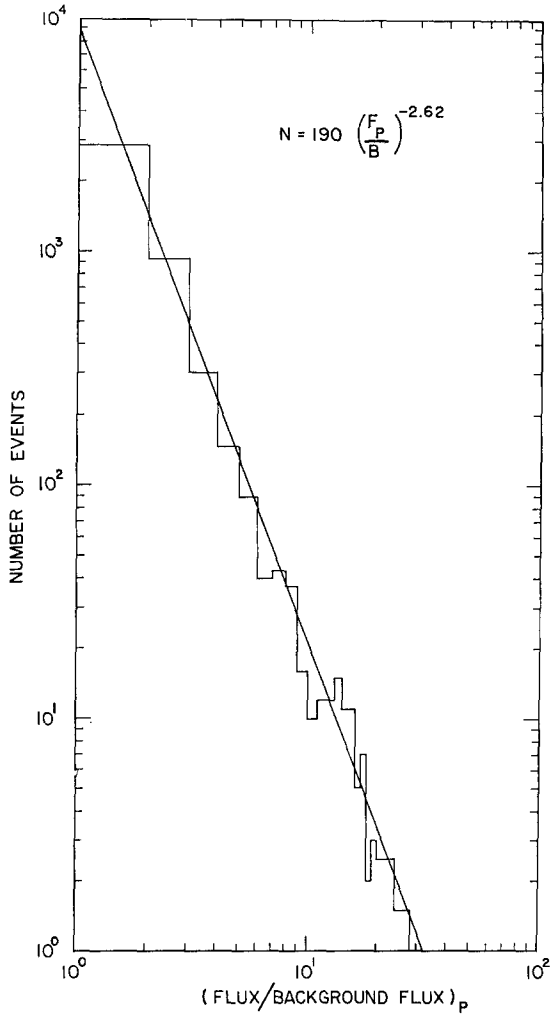

Fig. 8. Differential distribution of 2–12 Å X-ray bursts with respect to the ratio of the total observed flux to the background flux, evaluated at the time of peak burst intensity. The straight line is the least-squares fit over the region indicated.

resulting distribution is shown in Figure 8. The data can be well represented for four decades by the equation

$$N = 190(F/B)_p^{-2.62\pm0.01}, \tag{4}$$

where

$$(F/B)_p = \left(\frac{\text{total observed flux}}{\text{background flux}}\right)_{\text{maximum burst intensity}}$$

and N is the percentage of events occurring in the interval $(F/B)_p \pm 0.5$. This distribution could be fit more accurately by a simple empirical relation than any other studied.

Only 16% of the events have a ratio, $(F/B)_p$, of 4.0 or more. Such a minimum ratio value is adopted for the burst to be included in the listing of major solar X-ray flares published in the ESSA bulletin *Solar-Geophysical Data* (Van Allen, 1967b). Thus, 84% of the events represented in Figure 8 were not included in the published flare listings.

H. PEAK FLUX

The peak flux, F_p, is defined as

$$F_p = (F - B)_p . \tag{5}$$

There is the additional constraint that

$$(F/B)_p \geq 1.5 . \tag{6}$$

These two conditions combined restrict the peak flux values to

$$F_p \geq (B/2)_p . \tag{7}$$

For example, a peak flux value less than 1.0 milli-erg $(\text{cm}^2 \text{ sec})^{-1}$ cannot be recorded if the background flux exceeds 2.0 milli-erg $(\text{cm}^2 \text{ sec})^{-1}$. Thus the data analysis method used discriminates against low intensity bursts on the basis of the background flux value.

An attempt was made to correct for this effect by preparing a frequency of occurrence histogram for the background flux. The factor was then determined by which to normalize the number of events in each flux interval to a 100% frequency of background flux occurrence. The greatest correction factor used was 1.7 for the 0.0–1.0 milli-erg $(\text{cm}^2 \text{ sec})^{-1}$ interval.

A greater percentage of bursts tend to occur when the background flux level is higher. Since the number of events in the lower peak flux intervals was necessarily obtained during relatively quiet periods, it is probable that the correction applied does not provide enough of an increase for these events. It is believed that the number of events in the lower peak flux intervals may yet be too low.

The distribution obtained after correcting the data as described, again excluding any peak values observed on the edge of a data gap, is shown in Figure 9. There is an apparent peak in the distribution seen at a peak flux value of 1.0–2.0 milli-erg $(\text{cm}^2 \text{ sec})^{-1}$. The reality of this peak is not claimed; it is most likely due to the background flux and the selection problem.

The peak flux distribution can be approximated by a power law relation. Excluding the lowest peak flux interval, the equation for $1.0 \leqslant F_p \leqslant 100.0$ milli-erg $(\text{cm}^2 \text{ sec})^{-1}$ is

$$N = 59.9 \, F_p^{-1.66 \pm 0.02} , \tag{8}$$

where N is the percentage of bursts with peak flux F_p in the interval $F_p \pm 0.5$. The distribution falls below this curve at the higher peak flux values. If the second interval is excluded, using the peak flux range $2.0 \leqslant F_p \leqslant 100.0$ milli-erg $(\text{cm}^2 \text{ sec})^{-1}$, the equation is

$$N = 82.5 \, F_p^{-1.84 \pm 0.02} \tag{9}$$

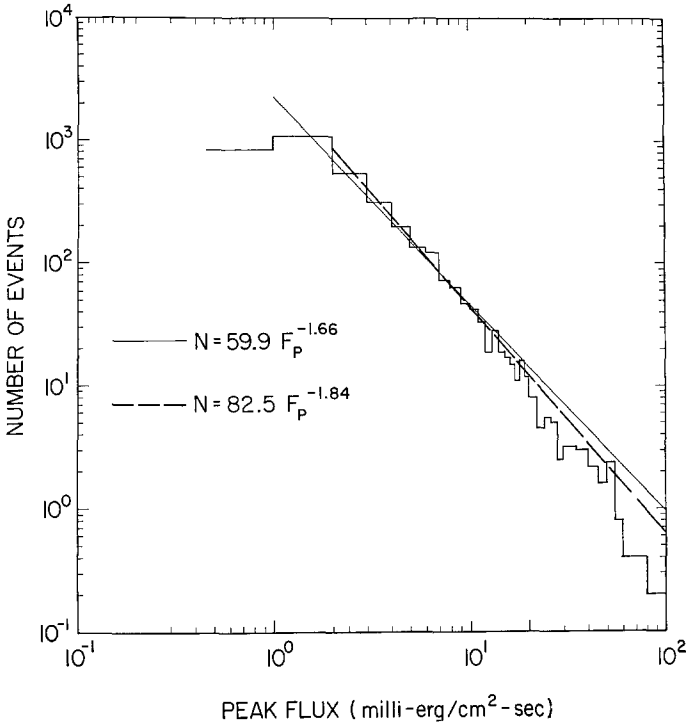

Fig. 9. Differential distribution of 2–12 Å X-ray bursts with respect to the peak burst flux. The straight lines are the least-squares fits over the regions indicated.

with the symbols retaining their previous definitions. These two equations represent 85% and 56% of the total number of events in Figure 9.

It is concluded that the distribution of bursts by peak flux can be represented by a power law relation with exponent -1.75 ± 0.1 over a range of two orders of magnitude in peak flux. At higher flux values the distribution falls off more rapidly than the given power law relation. There were only 14 bursts with peak flux greater than 100 milli-erg $(\text{cm}^2\ \text{sec})^{-1}$ in the time interval under consideration.

I. FLUX TIME INTEGRAL

The flux time integral distribution was constructed using only those events which had no data gaps during the event and for which the beginning and ending points were definitely known. (These points were unflagged.) The flux time integral was corrected for end contributions by the extrapolation method discussed in Section 3. In addition, the uncertainty discussed for the previous distribution concerning the number of events for smaller peak flux values must also affect the number of events for smaller flux time integral values. However, no correction was applied to the data, except that the lowest interval, 0.0–1.0 erg cm^{-2}, which should be most affected, was excluded from the distribution.

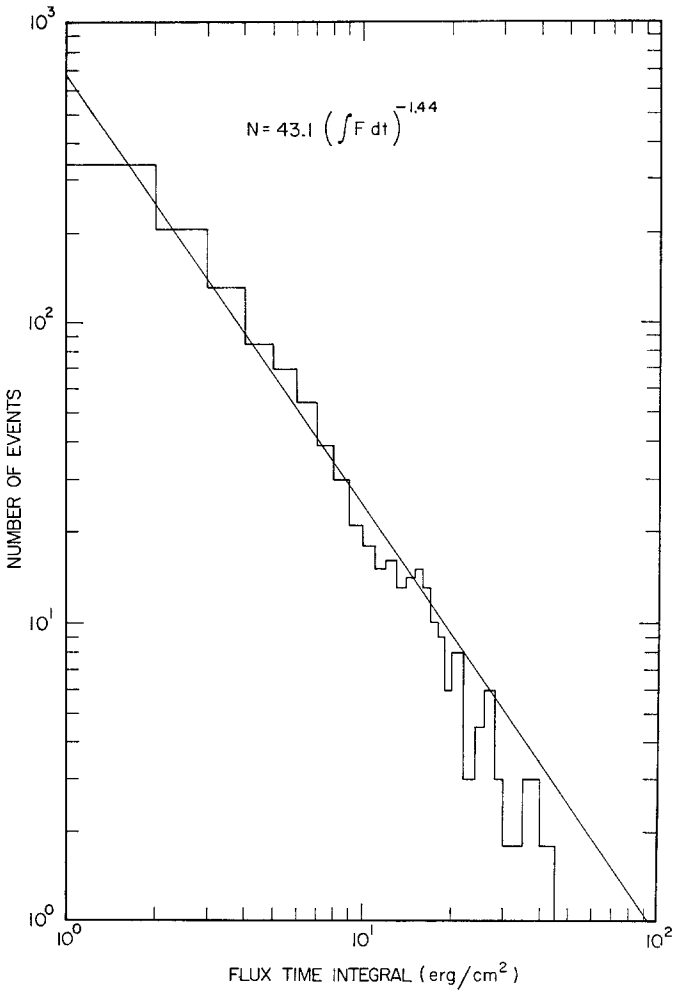

Fig. 10. Differential distribution of 2–12 Å X-ray bursts with respect to the value of the time integral of the burst flux for the duration of the burst and with end corrections added as described in the text (Section 3). The straight line in the least-squares fit over the region indicated.

The distribution of flux time integral values is presented in Figure 10. The distribution can be represented by

$$N = 43.1 \left(\int F \, dt \right)^{-1.44 \pm 0.01}, \tag{10}$$

where N is the percentage of events occurring with a flux time integral value, $\int F \, dt$ in erg cm^{-2}, in the interval $\int F \, dt \pm 0.5$.

J. DISCUSSION OF INTENSITY PARAMETERS

The examination of burst intensity parameters again indicates no more than one

primary class of burst. There is a smooth variation seen in all three distributions such that a power law relation can represent the data.

The concept of a solar X-ray burst arising from this study is of one standard form of event with the individuality of events owing to the departure of one or more parameters from their typical or most common values. The most common values might be the result of approximately the same physical conditions existing for the production of the majority of burst X-rays, while their departure from typical values might indicate the departure of one or more of the pertinent physical parameters in the emission region from its usual state. The true complexity of the flaring process is then manifested in the observed X-ray bursts.

5. Comparison with Hα Flares

The soft X-ray bursts were compared with Hα flares listed in *Solar-Geophysical Data* (1966–1969). An Hα flare and an X-ray burst were considered associated if either the start time of the two phenomena coincided within 5 min or if the peak flare and peak bursts times coincided within 10 min. Both confirmed and small or unconfirmed Hα flares were included in the study, the confirmed data being examined first. The relative occurrence statistics were determined, the dependence of peak X-ray flux upon flare importance was examined, and the heliographic longitude distributions of both Hα flares and soft X-ray bursts were studied.

A. RELATIVE OCCURRENCE STATISTICS

Of the 4028 X-ray bursts listed, 176 had uncertain peak times or occurred during periods of no Hα flare patrol. Of the remaining 3852 events, 70% could be associated unambiguously with Hα flares. This result agrees closely with the correlation of 69% between 7.7–12.5 keV bursts and Hα flares (Hudson *et al.*, 1969) but differs considerably from the correlation of 46% between 3.0–4.5 keV bursts with Hα flares (Culhane and Phillips, 1969). A correlation of 71–82% was found between 3 keV bursts and Hα by Harries (1968).

During the period under consideration in this study, 16468 Hα flares occurred. Hα flares occurring during periods of no X-ray data for several hours or more were excluded. Periods of no X-ray data of less than several hours occur more frequently and have no relationship to Hα flare occurrence. This will, however, affect the total percentage of Hα flares associated with X-ray bursts. The correlation of Hα flares (16468) with soft X-ray bursts (2698) is only 16%. This is very low compared to the values of 65% for Hα flares and 3.0–4.5 keV bursts (Culhane and Phillips, 1969) and 88% for Hα flares and 7.7–12.5 keV bursts (Hudson *et al.*, 1969).

The number of Hα flares accompanied by X-ray bursts depends strongly on the sensitivity of the X-ray detection method. The number of X-ray bursts increases strongly with decreasing peak X-ray flux. A factor of 3 or 4 increase in the number of X-ray bursts listed might be realized by decreasing the arbitrary burst identification criterion from 1.5 to 1.2 for the flux ratio to background at burst peak. Also, small

TABLE III

Results of detailed study of Hα flare and X-ray burst occurrences for March 1968

Hα importance	−F	−N	−B	1F	1N	1B	2F	2N	2B	Total
Hα flare with X-ray burst	16	45	10	4	8	6			1	90
Hα flare with unlisted but noticeable X-ray burst	103	93	14	2	1	3		1		217
Hα flare but no X-ray data	58	50	5	3	2	1				119
Hα flare with no detectable X-ray burst	55	38	2	1	2					98

bursts occurring during the rise or decay of a larger burst may be obscured and not listed. To illustrate these points, the data for the month of March 1968 was examined in detail.

The results of this comparison are presented in Table III. The four categories into which Hα flares were sorted are: an Hα flare accompanied by a listed X-ray burst; an Hα flare accompanied by an X-ray increase too small to be listed as a burst but still discernible by visual examination of the plotted data; an Hα flare during periods of no X-ray data coverage; and an Hα flare with no detectable X-ray burst. The dependence within each category on flare importance and the contrast between the total number of Hα flares accompanied by listed X-ray bursts and those accompanied by unlisted but noticeable X-ray bursts exemplify the strong dependence of the number of Hα flares accompanied by X-ray bursts on the X-ray burst sensitivity criterion. Furthermore, of 98 Hα flares with no detectable X-ray bursts, only 3 flares are of importance greater than a subflare. Figure 11 gives the X-ray data for the time during which one

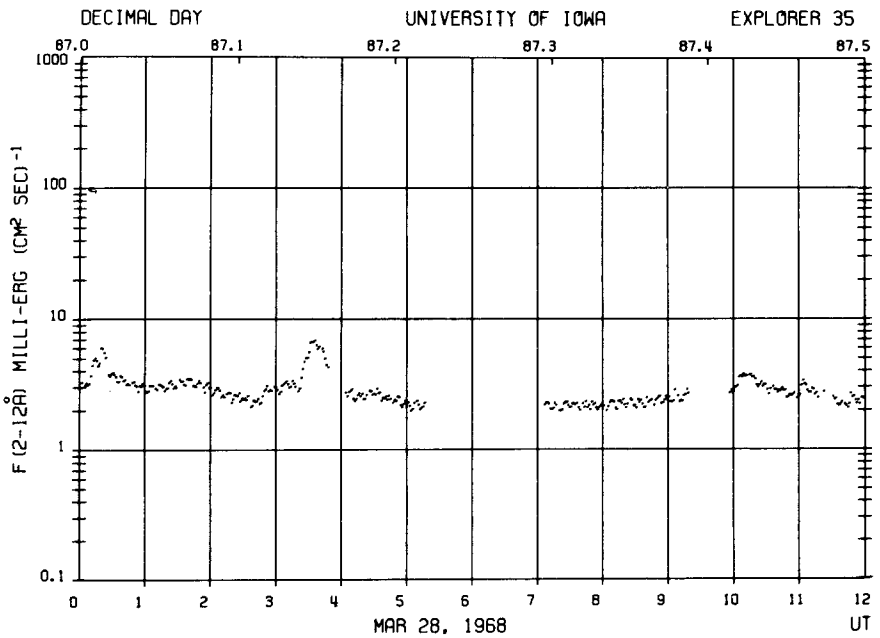

Fig. 11. Sample plot from the F (2–12 Å) catalog.

of the 1N Hα flares with no detectable X-ray bursts occurred. This confirmed flare started on 28 March 1968 at 0745, was at maximum phase as determined from area measurements at 0801, and ended at 0836. No X-ray enhancement greater than the statistical fluctuations in the data was seen during the entire time of the Hα flare.

The percentage association of Hα flares and listed X-ray bursts for March 1968 is then 17% or 22%, depending on whether the total number of Hα flares for the month or the number of Hα flares only during periods of X-ray coverage are used. If the

number of Hα flares accompanied by unlisted but noticeable X-ray bursts is included, the percentage association becomes 76%, using flare data only during periods of X-ray observations. The range of the percentage association is seen to be large and strongly dependent on the criteria used. This detailed comparison for March 1968 is thought to give typical, representative results. The mean value of the relative occurrence probability, shown in Figure 17, for the entire period July 1966 to September 1968 is 17%, the same as that for March 1968 when all Hα bursts were included.

The total number of X-ray bursts associated with each Hα importance classification as a function of the classification is shown in Figure 12. It is clear from this plot that

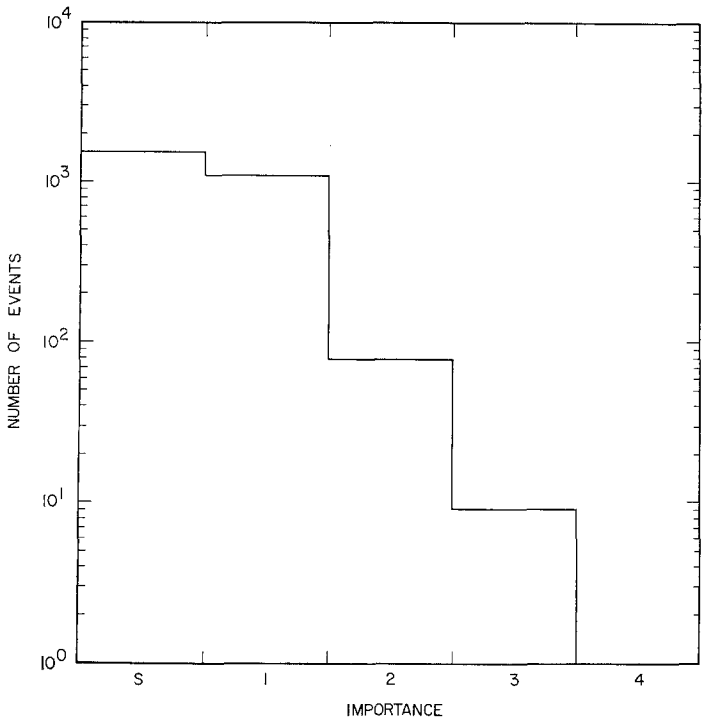

Fig. 12. Distribution of X-ray bursts which could be associated with Hα flares as a function of Hα flare importance.

the number of associated bursts follows the trend of Hα flares with an increasing number of events at decreasing flare importances, as Table III also shows.

It has been asserted previously that all Hα flares produce X-ray bursts (Teske, 1969; Hudson *et al.*, 1969). With the demonstrated dependence on sensitivity of the percentage association between Hα flares and X-ray bursts shown in this study, the assertion that all Hα events produce X-ray bursts is strongly supported.

B. AMPLITUDE RELATIONSHIP

The dependence of the X-ray burst peak flux on Hα importance was examined. The

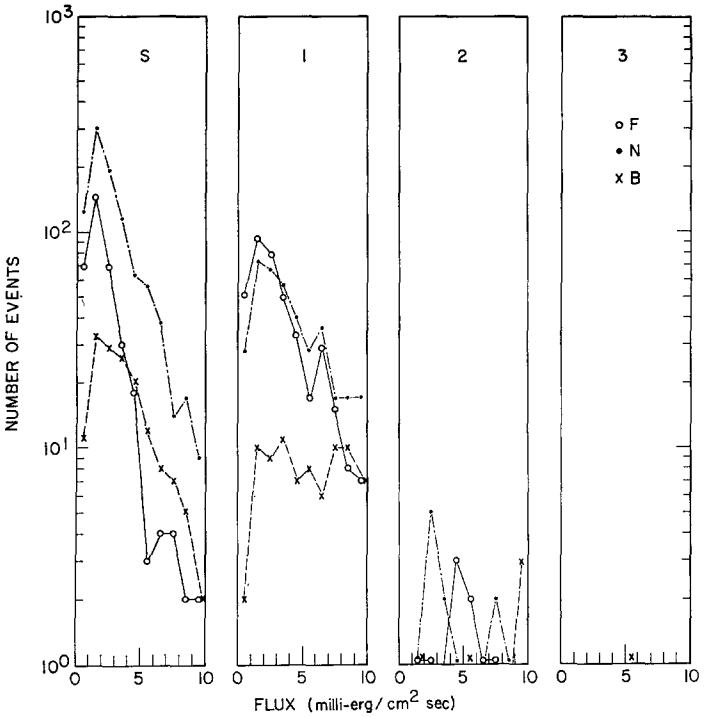

Fig. 13. Distribution of X-ray bursts which could be associated with Hα flares as functions of both the Hα flare importance and the peak burst flux, for peak burst fluxes less than 10.0 milli-erg $(cm^2\ sec)^{-1}$. The Hα flare importance by area is given at the top of each of the four plots while the relative intensity evaluations are indicated by different symbols and lines, as given on the fourth plot.

X-ray data were broken into two groups, those having a peak burst flux greater than, or less than, 10.0 milli-erg $(cm^2\ sec)^{-1}$. The data for the first group is shown in Figure 13. The most significant features of this plot are that there is a rapid increase in the number of X-ray bursts at smaller flare importances and that the number of X-ray bursts increases with decreasing peak flux value.

The plot of events with peak flux greater than 10.0 milli-erg $(cm^2\ sec)^{-1}$ shown in Figure 14 demonstrates a loose dependence of peak flux on flare importance. The largest peak flux value within an importance classification increases from F to N to B in each case except for importance 3, in which the statistics are not significant. Also, the largest peak flux in each classification increases in going from class to class at the same brightness level. The one exception to this trend is the high, circled point of 1N importance. This confirmed flare occurred on 6 July 1968 with maximum phase at 0956. This event, observed by ten stations, was reported as −N by three stations, as 1N by three, as 1B and 2F by one each, and 2B by two stations. The maximum flare times reported ranged from 0944 to 0957. On the basis of the wide variability in the optical reports of this flare, it is believed that the labeling of this flare as 1N is questionable, so that this one flare does not definitely disagree with the general trend of the

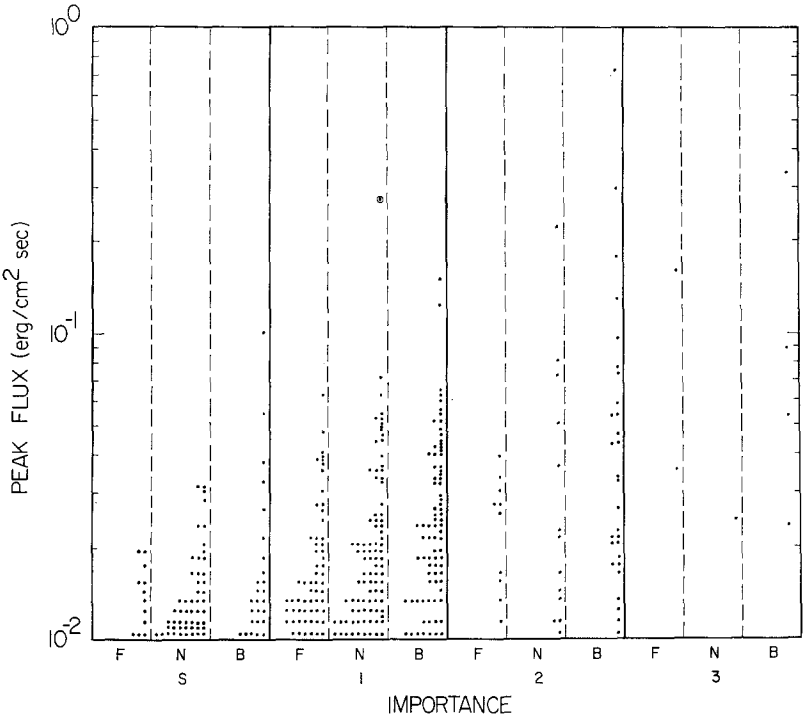

Fig. 14. Distribution of X-ray bursts which could be associated with Hα flares as functions of both the Hα flare importance and the peak burst flux, for peak burst fluxes greater than 10.0 milli-erg $(cm^2\ sec)^{-1}$.

data. There does appear a general increase in a gross sense, then, of the X-ray flux both with increasing flare area and with increasing relative intensity evaluation of the brightness. However, on an individual basis it is seen that at smaller flux values an X-ray burst could be produced by an Hα flare of any importance.

A plot of the median X-ray flux against flare importance is shown in Figure 15. This plot again shows a dependence of X-ray flux both on flare area and brilliance. The median burst flux increases both within a classification but with increasing brightness and from class to class at the same brightness. Statistics were insufficient to include the importance 3 data.

The general trend of increasing X-ray flux both with flare area and with flare brightness are shown by the data presented in this section. The increase in the number of X-ray bursts with decreasing flare importance is also evidenced by this data.

C. HELIOGRAPHIC LONGITUDE DEPENDENCES

The position on the solar disk of the source of an X-ray burst is assumed to be the same as that of the associated Hα flare. The 2698 X-ray bursts associated with Hα flares were examined to determine if any directionality exists in the X-radiation.

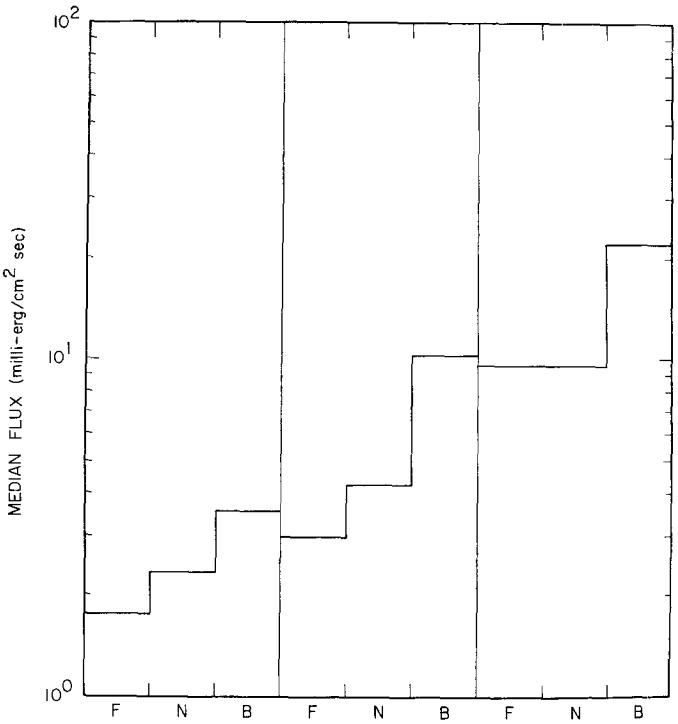

Fig. 15. Median burst flux 2–12 Å as a function of Hα flare importance.

The east-west symmetry of the X-ray sources was first examined, with the result that 1366 bursts occurred at east longitudes and 1332 occurred at west longitudes. These numbers indicate no east-west asymmetry.

The heliographic longitude distribution of X-ray bursts was next examined. The longitude distribution of University of Iowa observed 1–6 keV bursts has been studied by Ohki (1969) and Pinter (1969). On the basis of these and other X-ray data, they both conclude that directivity of the emission is present and both attribute the directivity to non-thermal bremsstrahlung produced by anisotropic, energetic electron streams.

Ohki (1969) finds the 1–6 keV burst occurrence uniform in longitude while Pinter (1969) claims a peak in the distribution at 30°–40° heliographic longitude. The 1–6 keV longitude distribution is the statistically most significant distribution either author uses, but they disagree on its form. Neither author takes into account explicitly the longitude distribution of the Hα flares against which the X-ray bursts were compared.

The number of Hα flares per 10° of heliographic longitude for the period July 1966 to September 1968 is shown in Figure 16. The error bars are $\pm\sqrt{N}$, N being the number of Hα flares in each 10° longitude interval. There is a significant decrease in the number of events at higher longitude values. There is also a weak peak in the distribution at 30°–40° longitude, just as found for the 1–6 keV burst longitude distribution (Pinter, 1969). These two distributions are very similar. It is clear that

care must be taken to properly take into account the Hα flare longitude distribution.

This was done by using the relative occurrence probability of X-ray bursts compared to Hα flares per 10° longitude. That is, the number of X-ray bursts per 10° of longitude was divided by the number of Hα flares which occurred in that same 10° interval. This should remove any Hα longitude dependence irregularities and leave only the X-ray burst longitude dependence in evidence. The results so obtained are shown in Figure 17. The mean value of the relative occurrence probability, 0.17, indicates that about 6 times as many Hα flares occur as do X-ray bursts. This point was discussed previously in this section where it was shown that this ratio is a strong function of the criteria of the X-ray burst identification process.

The error bars in Figure 17 were determined by the largest change possible in the ratio due to counting statistics. On this basis, some real variations do appear to occur at longitudes 70°–90°, as seen in Figure 16. This may be the result of the observational difficulty of assigning a longitude value to a flare at longitudes of 70°–90°. Also, flares

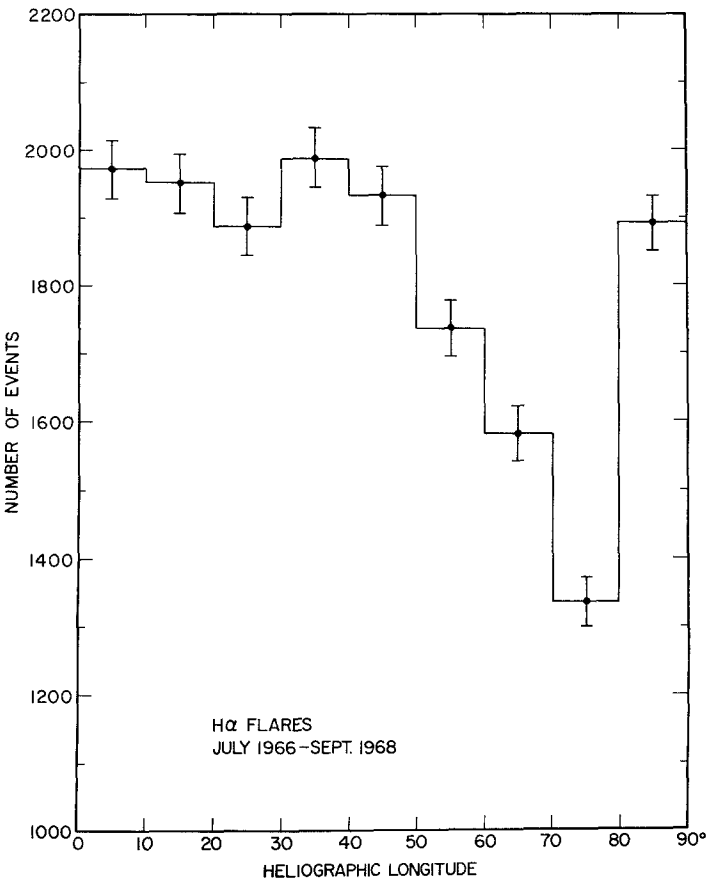

Fig. 16. Heliographic longitude distribution of Hα flares during the period July 1966 to September 1968 when X-ray data coverage was possible. Note suppressed zero at ordinate scale.

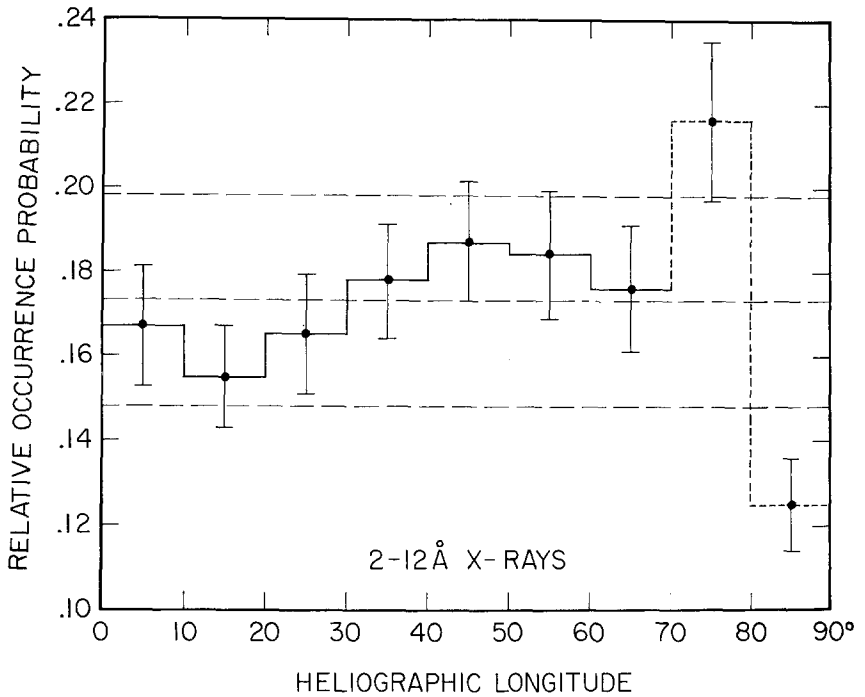

Fig. 17. Relative occurrence probability of 2–12 Å solar X-ray bursts with respect to Hα flares as a function of heliographic longitude for X-ray bursts observed from July 1966 to September 1968. Note suppressed zero of ordinate scale.

occurring up to 10° beyond the limb may be visible, increasing the number observed from 80°–90°, as seen in Figure 16. If, in Figure 17, the 70°–80° relative occurrence probability and the 80°–90° value are averaged, the average of the other 7 intervals is closely approached. For these reasons the variation in the X-ray burst relative occurrence probability longitude distribution at 70°–90° is thought not to reflect the X-ray longitude dependence and is therefore drawn as a heavy dashed line.

The central light dashed line is the mean value of the relative occurrence probability. The upper and lower dashed lines are one standard deviation from the mean value. All the relative occurrence probability values, except the 70°–90° values, lie within one standard deviation of the mean. There is a gradual rise to, and fall from, an apparent peak at 40°–50° in the distribution. However, in view of the error bars shown and the fact that all points, except 70°–90° lie within one standard deviation of the mean, this peak is thought not to be significant. This figure is taken to show that there is no significant directivity to the 1–6 keV X-radiation.

6. Comparison with Hard (>6 keV) X-Ray Bursts

The 1–6 keV burst X-ray flux recorded by Explorer 33 and Explorer 35 is insensitive to the spectral distribution of the X-radiation and provides only the magnitude of the

flux in this energy range. Both the magnitude and the spectral distribution must necessarily be known to examine quantitatively the observational data in terms of emission mechanisms. To this end a comparison of the 1–6 keV bursts was made with two different experimental observations of hard (photon energy > 6 keV) X-ray bursts.

A. COMPARISON WITH 10–50 KEV BURSTS

X-ray bursts in the energy range 10–50 keV were observed by the University of Minnesota Cosmic Ray Group with ionization chambers on the satellites OGO I and OGO III for the time interval 5 September 1964 to 31 December 1967. The cataloged form of these observations (Arnoldy *et al.*, 1968; Kane and Winckler, 1969) was used in a comparison study with the 1–6 keV bursts.

There were 134 hard X-ray bursts listed during times when University of Iowa equipment provided soft X-ray data. Accompanying soft X-ray bursts as listed by the burst program could be found for 100 of these hard X-ray bursts. The criterion for association was that the peaks coincide within ± 10 min.

Both the hard X-ray burst counting rate and the corresponding soft X-ray flux for a typical event are shown in Figure 18. The symbols shown are the data points through which the smoothed curves were drawn. The peak hard X-ray flux is seen to precede the peak soft X-ray flux, the soft X-ray event has a greater total duration than the

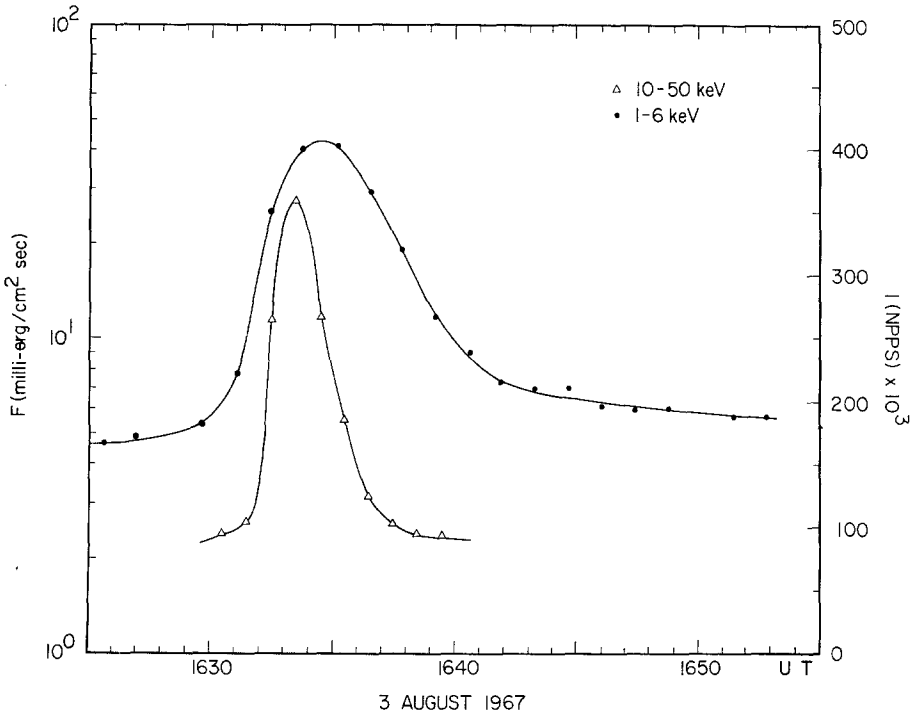

Fig. 18. Comparison plot between the soft (1–6 keV) X-ray flux (F) and the hard (10–50 keV) X-ray counting rate (I) as functions of time. Hard X-ray rate from Kane and Winckler (1969).

hard X-ray event, and the soft X-ray flux appears to initially begin to increase before the hard X-ray rate increases.

The time differences between the peaks of associated hard and soft X-ray bursts were examined. Soft X-ray bursts with an uncertain peak time were excluded from this study, leaving 86 good quality associated events. The number of events as a function of Δt, the time of the soft X-ray burst peak minus the time of the hard X-ray burst peak, is shown in Figure 19. It is seen that in nearly all events the hard X-ray peak occurs before the soft X-ray peak ($\Delta t > 0$). On the average the hard X-ray peak occurred 3 minutes before the soft X-ray peak.

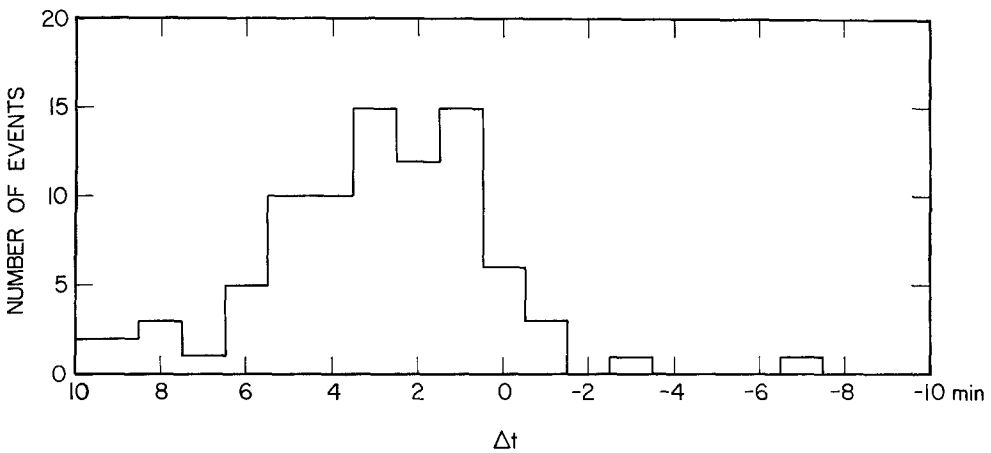

Fig. 19. Distribution of the associated 1–6 keV and 10–50 keV X-ray bursts according to the time difference, Δt, between the burst peaks. Δt is the time of the 1–6 keV peak minus the time of the 10–50 keV peak. Positive Δt results from the 10–50 keV peak occurring earlier than the 1–6 keV peak.

A delay in the time of maximum flux occurrence such that the peaks occur first with higher energy photons and then progressively for less energetic photons is in agreement with other observations. Culhane and Phillips (1969) find time differences of several minutes between 1–3 Å and 6–18 Å peaks. A delay of the order of 1 min between 0–3 Å and 0–8 Å peaks can be seen in the data presented by Kreplin *et al.* (1969). In each case the hardest peak occurs first.

If the radiation were due to free-free emission from a region with a constant emission measure, the peak should occur simultaneously at all energies. Since this is not what is observed, by at least three independent groups, free-free emission with a constant emission measure must not be the case.

Another test of the possibility of free-free emission with a constant emission measure is an examination of the relationship of the hard and soft X-ray peak fluxes. According to theory, there should be a unique correspondence between the two peak fluxes at a given temperature. The 1–6 keV peak flux was plotted against the 10–50 keV peak counting rate, as shown in Figure 20, to test this prediction. Again only soft X-ray

bursts with well-defined peak times were used. The straight line in Figure 20 was arbitrarily drawn to demonstrate that a power law relationship could approximately fit the data. It is worth noting the wide range of values found in this data sample, nearly 3 orders of magnitude in the soft X-ray flux and nearly 5 orders of magnitude in the hard X-ray counting rate. Also to be noted is that the departure of the individual data points from a straight line fit is independent of the size of the soft X-ray flux or of the hard X-ray counting rate; no systematic departures are seen.

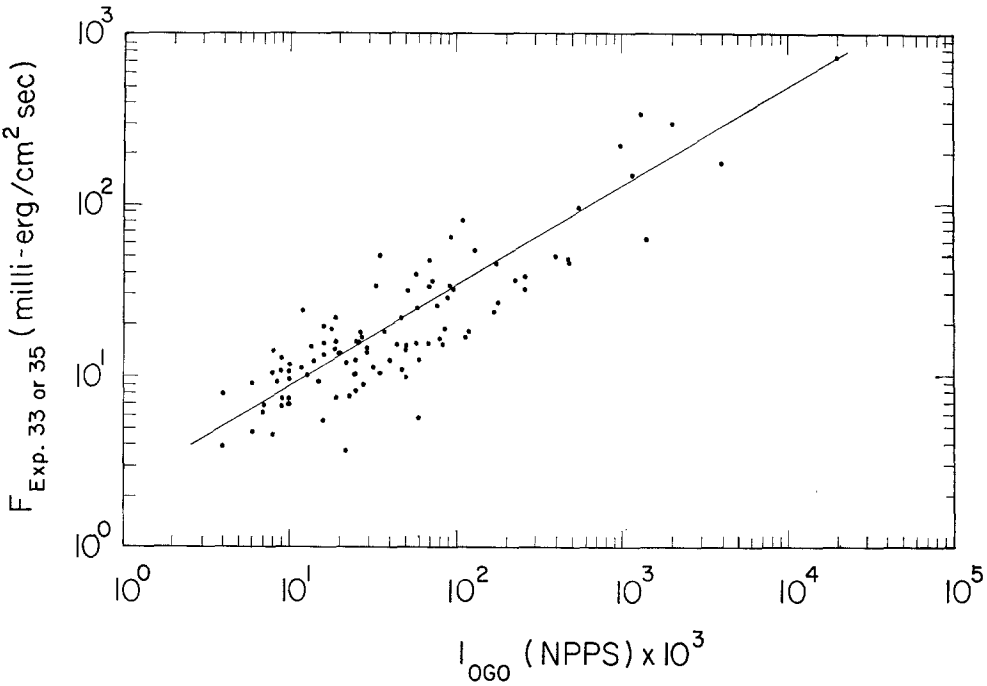

Fig. 20. Peak flux of the 2–12 Å bursts as a function of the peak excess ion chamber rate due to corresponding 10–50 keV X-ray bursts. The latter rates were taken from Arnoldy *et al.* (1968) and Kane and Winckler (1969).

To examine this peak flux relationship quantitatively, the free-free emission formula must be integrated with the appropriate detector response functions. To obtain the ionization chamber counting rate due to free-free emission, the response curve given by Kane (1967) was integrated with the free-free expression.

For the Explorer detector the response is effectively constant throughout the bandwidth. The observed quantity as used in this study is the flux in the 2–12 Å range given by Equation (1).

The experimentally determined ratio of 10–50 keV peak X-ray counting rate to 1–6 keV peak X-ray flux plotted against the 1–6 keV peak flux is shown in Figure 21. The data points represented by triangles had a peak separation of ± 2 min or less;

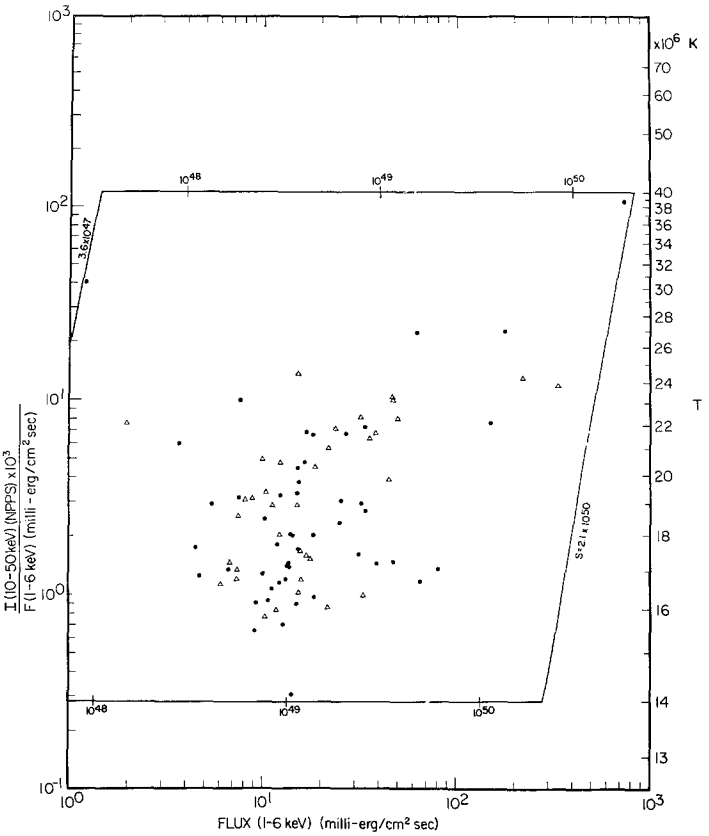

Fig. 21. Ratio of the 10–50 keV peak counting rate to the 1–6 keV peak flux as a function of the 1–6 keV peak flux. The temperatures to which these ratios correspond, assuming free-free emission, are given on the right-hand scale. The horizontal lines in the plot correspond to the behavior expected due to a constant temperature decay with only the emission measure changing; various emission measures are ticked in. The near vertical lines correspond to a decay with constant emission measure and changing temperature only. Data points represented by triangles had a peak separation of $\pm$ 2 minutes or less; filled circles had a difference of more than $\pm$ 2 minutes. Hard X-ray rates from Arnoldy *et al.* (1968) and Kane and Winckler (1969).

those represented by solid circles had a difference of more than $\pm$ 2 min. There is no separation of the data on this parameter.

The results of this study are that the emission measure is neither constant within an event (temporal study) nor from event to event (amplitude study). If the theory of free-free emission is assumed, the temperature is in the range 14–39 $\times 10^6$ K and the emission measure is in the range $3.6 \times 10^{47} - 2.1 \times 10^{50}$ cm^{-3}.

B. COMPARISON WITH 7.7–12.5 KEV BURSTS

X-ray bursts in the energy ranges 7.7–12.5 keV and 12.5–22.0 keV were observed by use of a collimated scintillation counter with spectrum analysis on the OSO III satellite by the University of California, San Diego (Hudson *et al.*, 1969).

From a list of 37 events in the 7.7–12.5 keV range during periods when soft X-ray data coverage existed, 18 corresponding bursts were found in the computer listing of soft X-ray bursts. The largest soft X-ray peak flux was $\sim$ 6 milli-erg $(\text{cm}^2\ \text{sec})^{-1}$, quite small compared to the fluxes used in the previous study. The 19 unassociated hard X-ray bursts were for the most part accompanied by soft X-ray events too small to be classified as bursts by the criterion used. Thus, this sample is composed of small events.

The ratio of the peak 7.7–12.5 keV flux to the peak 1–6 keV flux as a function of the 1–6 keV flux for these 18 events is shown in Figure 22. The ratio of these fluxes has again been calculated assuming free-free emission from an isothermal volume. The range of temperatures indicated by these data is 12–18 $\times 10^6$ K. The range of soft X-ray fluxes is so small that a constant emission measure might be said to fit the data to within a factor of 3. However, the fit is not good to a factor of 2 and the possibly constant (within a factor of 3) emission measure might be the result of using too limited a range of flux values. The conclusion drawn from Figure 22 is that the emission measure is not constant to within a factor of 2 from event to event.

The ratio of 7.7–12.5 keV flux to 1–6 keV flux plotted against the 1–6 keV flux during

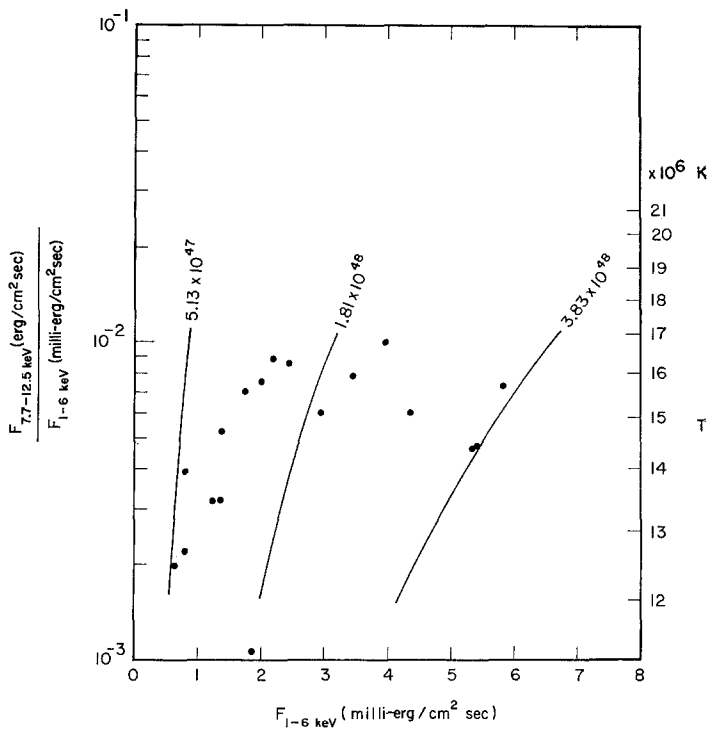

Fig. 22. Ratio of 7.7–12.5 keV burst flux to 1–6 keV peak flux as a function of 1–6 keV peak flux. The temperatures corresponding to these ratios, assuming free-free emission, are given on the right hand scale. Lines corresponding to given constant emission measures and changing temperature only are drawn through the data. The hard (7.7–12.5 keV) X-ray fluxes are courtesy of Hudson *et al.* (1969).

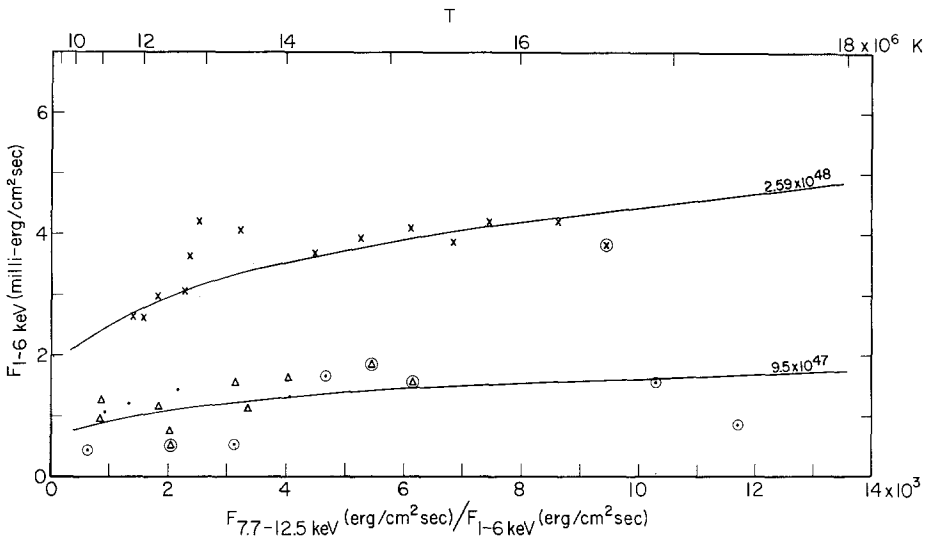

Fig. 23. Soft (1–6 keV) flux versus the ratio of 7.7–12.5 keV flux to 1–6 keV flux during three individual events. The three events are distinguished by the three different symbols. Circled points occurred before the peak in the 1–6 keV flux. Temperatures to which these ratios correspond, assuming free-free emission, are given along the upper axis. Two curves of given constant emission measure and changing temperature only are drawn through the data. Hard (7.7–12.5 keV) X-ray fluxes courtesy of Hudson *et al.* (1969).

three arbitrarily chosen events is shown in Figure 23. The three different events are denoted by different symbols. The circles around particular symbols indicate ratios occurring before the peak of the soft X-ray event. In general, points move toward higher temperatures during the rise of the event and toward lower temperatures during the decay phase. Two curves corresponding to given constant emission measures and the indicated temperatures have been drawn through the data to facilitate comparison of the experimental data with theory. It is seen that the emission measure describing the two bursts is less than one-half the emission measure describing the third burst. Again the emission measure is seen to be not constant to within a factor of 2. Also within an event, individual data points depart from the theoretical curve by more than a factor of 2, after including the experimental uncertainties.

One of the three events shown on Figure 23 is shown on an expanded scale in Figure 24. The emission measure has been calculated at each point. The arrows are in the direction of increasing time within the event. The change of both emission measure and temperature during the event are clearly displayed. The emission measure is consistently lower during the increasing temperature phase and gradually increases with decreasing temperature. The variation of the emission measure within the event is also supported by the fact that for the 18 events shown in Figure 22, the 7.7–12.5 keV peak flux occurred an average of 3 min before the 1–6 keV peak flux.

The comparison with 7.7–12.5 keV bursts reveals that the emission measure is

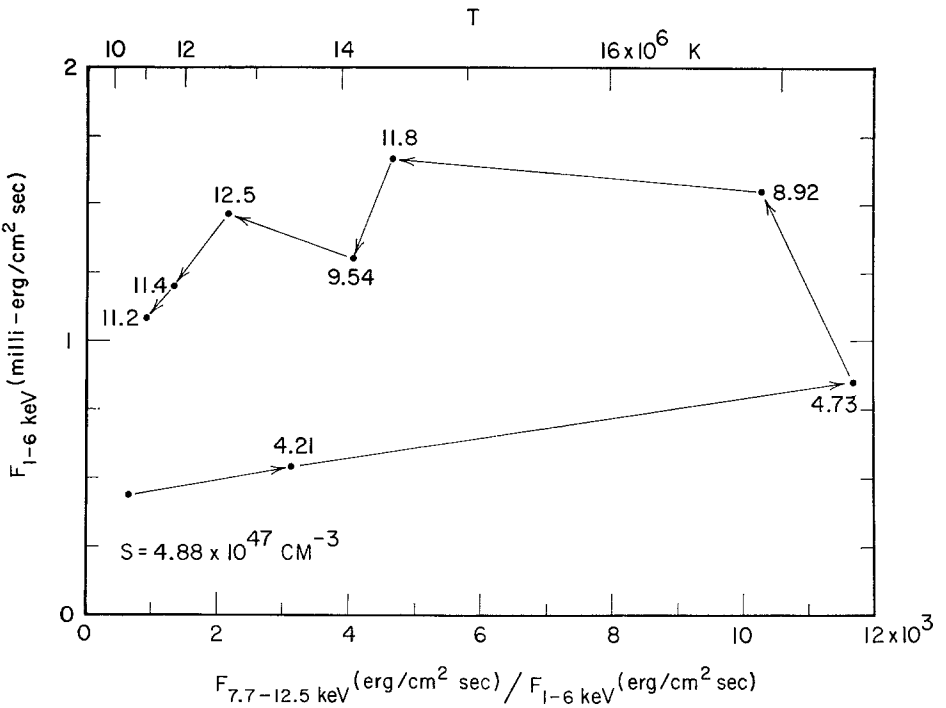

Fig. 24. Soft (1–6 keV) flux versus the ratio of 7.7–12.5 keV flux to 1–6 keV flux during an individual event. Temperatures to which these ratios correspond, assuming free-free emission, are given along the upper axis. The emission measure calculated using free-free emission, the observed 1–6 keV flux, and the temperature obtained from the ratio are given with each point. The arrows connect successive points in time as the event progressed. Hard (7.7–12.5 keV) X-ray fluxes courtesy of Hudson *et al.* (1969).

neither constant (within a factor of 2) within an event nor from event to event. Temperatures of $12–18 \times 10^6$ K and emission measures of $4.9 \times 10^{47} - 3.8 \times 10^{48}$ cm^{-3} for free-free emission account for the data.

C. DISCUSSION OF COMPARISON RESULTS

The result of the comparison of the soft X-ray bursts with both the 10–50 keV bursts and the 7.7–12.5 keV bursts consistently show that the emission measure in a free-free emission mechanism explanation of the radiation is constant neither within an event nor from event to event.

These results would be invalidated if the emission mechanism for X-ray bursts in one of the energy ranges used were not free-free emission. Either the hard X-ray bursts might be attributed to non-thermal bremsstrahlung or the soft X-ray bursts to predominantly a line emission process. Kane (1969) has shown that hard X-ray bursts are composed of two components. One component is impulsive in nature, has a very short total duration ($\sim$30 sec), and is attributed to non-thermal bremsstrahlung. The other component reaches a maximum later in the event, has a greater duration (5–10

min), and has a steeper photon energy spectrum. This component has many properties marking it as thermal in origin, which it is assumed to be. The hard X-ray bursts used in this study were then most likely composed of this thermal component as the predominant component due to the longer duration ($\sim$5–10 min) of the 10–50 keV bursts. On this basis the hard X-ray bursts used in this study are thought to be of thermal origin.

Line emission is thought to not contribute substantially to the 1–6 keV burst flux for the following reasons. Meekins *et al.* (1968) from crystal spectrometer data found that the continuum from 1–10 Å during solar flares always dominated the line emission by more than an order of magnitude. Data presented by Rugge and Walker (1968) show that shortly after two class 1 flares the continuum dominated the lines in the wavelength range 7–12 Å. Spectra presented by Neupert *et al.* (1967) also show that in the wavelength range 2–12 Å during flares the continuum emission dominated the line emission.

On theoretical grounds, calculations performed by Gibson (1969) show that for temperatures greater than $\sim 6 \times 10^6$ K free-free emission exceeds both free-bound and bound-bound emission, including the effects of dielectronic recombination. In addition, the free-bound emission is always greater than the bound-bound contribution. The calculations of Culhane (1969) for free-free and free-bound thermal continuum radiation show that in the wavelength interval 2–12 Å free-free dominates free-bound emission for temperatures greater than $\sim 8 \times 10^6$ K. Since the free-bound exceeds the bound-bound emission, free-free emission then dominates at temperatures greater than $\sim 8 \times 10^6$ K. Thus both on experimental and theoretical grounds, line emission is thought to not contribute significantly to the 1–6 keV burst flux and free-free emission thus appears to be the dominant mechanism.

The temperatures and emission measures obtained by attributing X-ray bursts in the 1–50 keV range to free-free emission are in the range of values for these parameters obtained by a number of workers. Chubb *et al.* (1964) found a temperature of about 10^7 K from the slope of the photon spectrum for energies from 2–4 keV during times of subflare activity. Meekins *et al.* (1968) derived temperatures of $15–20 \times 10^6$ K from the slope of the photon spectrum from 3.3–8.5 Å during solar flares ranging from class 1 to class 3. Hudson *et al.* (1969) found temperatures in the range $10–50 \times 10^6$ K for solar X-ray bursts in the energy range 7.7–22.0 keV. Neupert (1968) finds consistency between the 1.87 Å line emission and a model in which the temperature is in the range $20–40 \times 10^6$ K. Culhane and Phillips (1969) determined temperatures of $10–30 \times 10^6$ K for impulsive X-ray bursts at energies less than 10 keV observed with instruments on OSO IV.

Thus agreement is emerging on temperatures of $10–40 \times 10^6$ K as the range during solar flares, in agreement with the present work, with free-free emission being the dominant process. The nonconstancy of the emission measure during an event is necessary to account for the more energetic photon peak fluxes occurring before the less energetic photon peak fluxes. From event to event the emission measure also changes as evidenced by the analysis presented here.

The flare concept emerging from this study is that a small region is first quickly heated and then loses energy to surrounding regions such that the temperature attained in the larger region is $10\text{–}40 \times 10^6$ K. The same process occurs for all flares but the exact conditions differ from event to event to cause the apparent individuality of bursts. As energy is lost from the hot core, the effective emission measure changes. The flare model of Carlquist (1968) does provide a sufficiently rapid acceleration in a sufficiently small volume and with a large enough energy release to account for the production of the hot core. This hot core would be the source of non-thermal electrons needed to cause rapid excitation of energetic iron lines observed to occur first in an event and to then be followed by the occurrence of less energetic lines. Some of the non-thermal electrons would emit the microwave impulsive burst, depending on their position in the magnetic field, etc. Others would thermalize, producing the heating needed to create the observed X-ray emission. Such a flare model is consistent with the observational facts and is in agreement with the models suggested by Meekins *et al.* (1968) and by Neupert (1968).

7. Conclusions

The conclusions of this paper are:

(1) The most frequently occurring rise time (20% to peak burst intensity) for 2–12 Å solar X-ray bursts is 4 min. The most common decay time is 12 min; the most common total duration is 16 min.

(2) The differential rise time distribution can be represented by an exponential law with exponent -0.1004 ± 0.0009 for rise times of 4 min or greater.

(3) The differential distribution of the ratio of rise time to decay time has a maximum at 0.3. From a ratio of 0.3 to 2.7 the distribution can be represented by an exponential law with exponent -2.31 ± 0.02.

(4) The differential distribution of the ratio of rise time to total burst duration has a maximum at 0.25.

(5) The differential distribution of the ratio of the total observed flux to the background flux at the burst peak can be represented by a power law with exponent -2.62 ± 0.01 for $1.5 < (F/B)_p < 32$.

(6) The differential distribution of the peak burst fluxes can be represented by a power law with exponent -1.75 ± 0.1 over the range 1–100 milli-erg $(\text{cm}^2\ \text{sec})^{-1}$.

(7) The differential distribution of the flux time integral values can be represented by a power law with exponent -1.44 ± 0.01 over the range 1–50 erg cm^{-2}.

(8) The number of Hα flares that can be correlated with X-ray bursts is strongly dependent on the intensity criterion of the X-ray burst identification scheme. Detailed consideration gives strong support to the belief that all Hα events produce X-ray bursts. The correlation of X-ray bursts with Hα flares is $\sim 70\%$.

(9) A general tendency for larger peak X-ray fluxes to occur with both larger flare areas and with brighter events is found.

(10) The heliographic longitude dependence of Hα flares from July 1966 to Sep-

tember 1968 is found to be non-uniform. However, the *relative* occurrence probability of 2–12 Å X-ray bursts (properly taking into account the non-uniformity of the Hα flare distribution) is found to be independent of heliographic longitude. This result detracts from proposals that a significant portion of the X-radiation is due to non-thermal bremsstrahlung from energetic electrons moving in preferred geometries.

(11) The ratio of 1–6 keV to 10–50 keV burst peaks, assuming free-free emission for the X-ray burst production, yields temperatures of $14\text{–}39 \times 10^6$ K and corresponding emission measures of 3.6×10^{47} cm^{-3} to 2.1×10^{50} cm^{-3}. The emission measure was found to vary both during individual events and from event to event.

(12) In a similar manner, ratios formed with 7.7–12.5 keV and 1–6 keV burst peaks yield temperatures of $12\text{–}18 \times 10^6$ K and corresponding emission measures of 4.9×10^{47} to 3.8×10^{48} cm^{-3}. The emission measure was again found to vary, both from event to event and during individual events, by more than a factor of 2.

(13) The burst data studied in the range 1–50 keV are consistent with a free-free emission mechanism with temperatures of $12\text{–}39 \times 10^6$ K and an emission measure which varies both during an event and from event to event from 3.6×10^{47} cm^{-3} to 2.1×10^{50} cm^{-3}.

Acknowledgements

The author wishes to thank Professor James A. Van Allen for making Explorer 33 and Explorer 35 data available to him and for guidance and suggestions during the course of the work with which this paper is concerned. Dr. J. Neff is thanked for helpful discussions and interest in this topic. Sister Jean Gibson, O.S.B., is thanked for help rendered in the development and execution of the data reduction method. The assistance of E. Sarris with the data analysis is appreciated, as is the assistance of P. Dylhoff with the computer program.

The author is indebted to Drs. H. S. Hudson, L. E. Peterson, and D. A. Schwartz of the University of California at San Diego for the use of their 7.7–12.5 keV X-ray burst data in Section 6B of this paper.

Support for this work has been provided at various stages by contract NAS5-9076 with the Goddard Space Flight Center, by National Aeronautics and Space Administration grant NGL 16-001-002, and by contract No. N00014-68-A-0196-0003 with the Office of Naval Research. During the various phases of this work, the author was the recipient of a National Aeronautics and Space Administration Traineeship and of a U.S. Steel Graduate Research Fellowship.

References

Arnoldy, R. L., Kane, S. R., and Winckler, J. R.: 1968, 'An Atlas of 10–50 keV Solar Flare X Rays Observed by the OGO Satellites 5 September 1964 to 31 December 1966', University of Minnesota Cosmic Ray Technical Report CR-108, January 1968.

Carlquist, P.: 1968, 'Solar Flares Caused by High Impedance Regions in Current Filaments', Royal Institute of Technology Research Report No. 68-11, Stockholm, May 1968.

Chubb, T. A., Friedman, H., and Kreplin, R. W.: 1964, 'Spectrum of Solar X-Ray Emission from 2–20 keV during Subflare Activity', in P. Muller (ed.), *Space Res.* **4**, 759.

Culhane, J. L.: 1969, 'Thermal Continuum Radiation from Coronal Plasmas at Soft X-Ray Wavelengths', *Monthly Notices Roy. Astron. Soc.* **144**, 375.

Culhane, J. L. and Phillips, K. J. H.: 1969, 'Solar X-Ray Bursts at Energies Less Than 10 keV Observed with OSO 4', Mullard Space Science Laboratory Research Report, University College, London.

De Jager, C. and Kundu, M. R.: 1963, 'A Note on Bursts of Radio Emission and High Energy (> 20 keV) X-Rays from Solar Flares', in P. Muller (ed.), *Space Res.* **3**, 836.

Drake, J. F.: 1970, 'Soft Solar X-Ray Burst Characteristics', University of Iowa Research Report 70-1, January 1970.

Drake, J. F., Gibson, Sr. J., O.S.B., and Van Allen, J. A.: 1969, 'Iowa Catalog of Solar X-Ray Flux (2–12 Å)', *Solar Phys.* **10**, 433.

Elwert, G.: 1968, 'The Significance of the Polarization of Solar Short-Wavelength X-Rays', in K. O. Kiepenheuer (ed.), 'Structure and Development of Solar Active Regions', *IAU Symp.* **35**, D. Reidel, Dordrecht, Holland.

Gibson, Sr. J., O.S.B.: 1969, 'The Correlation of X-Ray Radiation (2–12 Å) with Microwave Radiation (10.7 cm) from the Non-Flaring Sun', Ph.D. Thesis, University of Iowa, Iowa City, Iowa.

Harries, J. R.: 1968, 'Variable X-Ray Fluxes from Celestial Objects', Ph.D. Thesis, University of Adelaide, South Australia.

Hudson, H. S., Peterson, L. E., and Schwartz, D. A.: 1969, 'The Hard Solar X-Ray Spectrum Observed from the Third Orbiting Solar Observatory', *Astrophys. J.* **157**, 389.

Kane, S. R.: 1967, 'Application of an Integrating Type Ionization Chamber to Measurements of Radiation in Space', University of Minnesota Cosmic Ray Technical Report CR-106.

Kane, S. R.: 1969, 'Observations of Two Components in Energetic Solar X-Ray Bursts', *Astrophys. J.* **157**, L139.

Kane, S. R. and Winckler, J. R.: 1969, 'An Atlas of 10–50 keV Solar Flare X-Rays Observed by the OGO Satellites 1 January to 31 December 1967', University of Minnesota Cosmic Ray Technical Report CR-134, April 1969.

Kreplin, R. W., Moser, P. J., and Castelli, J. P.: 1969, 'Flare X-Ray and Radio Wave Emission', paper presented at the XIIth Plenary Meeting of COSPAR, Prague, Czechoslovakia, May 1969.

Meekins, J. F., Kreplin, R. W., Chubb, T. A., and Friedman, H.: 1968, 'X-Ray Line and Continuum Spectra of Solar Flares from 0.5 to 8.5 Angstroms', *Science* **162**, 891.

Neupert, W. M.: 1968, 'Comparison of Solar X-Ray Line Emission with Microwave Emission during Flares', *Astrophys. J.* **153**, L59.

Neupert, W. M., Gates, W., Swartz, M., and Young, R.: 1967, 'Observation of the Solar Flare X-Ray Emission Line Spectrum of Iron from 1.3 to 20 Å', *Astrophys. J.* **149**, L79.

Ohki, K. I.: 1969, 'Directivity of Solar Hard X-Ray Bursts', *Solar Phys.* **7**, 260.

Pinter, S.: 1969, 'Longitudinal Distribution of X Bremsstrahlung on the Solar Disk', *Solar Phys.* **8**, 142.

Rugge, H. R. and Walker, A. B. C., Jr.: 1968, 'Solar X-Ray Spectrum below 25 Å', in A. P. Mitra, L. G. Jacchia, and W. S. Newman (eds.), *Space Res.* **8**, 439.

Solar-Geophysical Data, issued by the Institutes for Environmental Research, U.S. Department of Commerce, Nos. 264–295, August 1966–March 1969.

Takakura, T. and Kai, K.: 1966, 'Energy Distribution of Electrons Producing Microwave Impulsive Bursts and X-Ray Bursts from the Sun', *Publ. Astron. Soc. Japan* **18**, 57.

Teske, R. G.: 1969, 'Observation of the Solar Soft X-Ray Component; Study of its Relation to Transient and Slowly-Varying Phenomena Observed at Other Wavelengths', *Solar Phys.* **6**, 193.

Van Allen, J. A.: 1967a, 'The Solar X-Ray Flare of July 7, 1966', *J. Geophys. Res.* **72**, 5903.

Van Allen, J. A.: 1967b, 'Catalog of Solar X-Rays', *Solar-Geophysical Data*, issued by the Institutes for Environmental Research, U.S. Department of Commerce, July 1967–August 1969.